Mausam, (1992), **43**, 3, 259-268

551.513.1 : 551.510.522 : 551.509.333

Numerical simulation of a tropical storm boundary layer

J.C. MANDAL

Regional Meteorological Centre, Calcutta

(*Received 6 March 1987*)

सार—उष्णकटिबंधीय तूफान के सतह परिसीमा स्तर के अध्ययन के लिए एक निदेश अभिकल्पित किया गया। संख्यात्मक पद्धति में परिमित अंतर द्वारा समकालिक अरैखिक अवकल समीकरण के दो सिस्टम के लिए दो स्तरीय परिसीमा मूल्य समस्या का समाधान है। उष्णकटिबंधीय तूफान परिसीमा स्तर के आन्तरिक और बाहरी दोनों क्षेत्रों में प्रवाह को प्रस्तुत करने के लिए उपयुक्त स्ट्रोक के स्ट्रीम फंक्शन विकसित किए गए हैं। इस पद्धति का लाभ यह है कि अरैखिक र्म्स् की उपेक्षा किए बिना तूफान के केन्द्र के बाहरी क्षेत्र से आरम्भ होने वाले उष्णकटिबंधीय तूफान की परिसीमा स्तर का अध्ययन किया जा सकता है। इसके अतिरिक्त और स्पर्शीय और त्रिज्य वेगों के लिए ऊर्ध्वाधर प्रोफाइल के पूर्वानुमानों की कोई आवश्यकता नहीं है। यह पद्धति स्थायी है और कुछ पुनरावृति के साथ अभिमुख होती है। घर्षण स्तर के ऊपर प्रवाह प्रवण संतुलन में स्थायी सममिति अक्ष भ्रमिल द्वारा प्रस्तुत किया गया है। परिसीमा स्तर की विशेषताओं पर विक्षोभ के प्रभाव का पता लगाने के लिए स्लिप परिसीमा स्थितियों के बिना विस्कासिता के भंवर गुणांक की चार विभिन्न स्थितियों द्वारा विक्षोभ को प्रस्तुत किया गया है। ऊर्ध्वाधर दिशा में 40 ग्रिड बिन्दु को लेते हुए परिकलन किया गया है। यह देखा गया है कि यदि परिसीमा स्तर पर अध्यारोपित प्रवाह के साथ विस्कासिता की भंवर गुणांक परिवर्तित समझे जाते हैं तो प्रेक्षणों के साथ ये विलयन सही रूप से बठते हैं। ये विलयन परिसीमा स्तर के आन्तरिक क्रोड से बहिर्वाह भी दर्शाते हैं जो कि तूफान की आँख के सृजन के लिए आवश्यक है।

ABSTRACT. A model has been designed to study the surface boundary layer of a tropical storm. The numerical method consists of solving a two point boundary value problem for two systems of simultaneous non-linear differential equations by finite differences. A Stoke's stream function suitable to represent the flow both in interior and exterior regions of a tropical storm boundary layer has been developed. The advantage of the method is that the boundary layer of the tropical storm can be studied starting from the outer region to the centre of the storm without neglecting non-linear terms. In addition, there is no need for assumptions on the vertical profiles for tangential and radial velocities. The method is stable and converges within a few iterations. The flow above the friction layer is represented by a steady axisymmetric vortex in gradient balance. To investigate the effect of turbulence on boundary layer characteristics, turbulence has been represented by four different variations of the eddy coefficient of viscosity with no slip boundary conditions. Computations have been performed taking 40-grid points in the vertical direction. It is observed that, if the eddy coefficient of viscosity is assumed to vary with the superimposed flow above the boundary layer, the solutions compare favourably well with observations. The solution also shows an outflow from the inner core of the boundary layer which is necessary for creation of an eye of the storm.

Key words — Boundary layer, Tropical storms, Axisymmetric vortex

1. Introduction

Observational data on tropical storm are still fragmentary because their formation and subsequent motion are over tropical oceans, where few observations exist. Although the large scale features of a tropical storm are now well known, only the relatively dominant tangential flow is well documented. In case studies, there is no sufficient data density to allow an accurate determination of other parameters; as such, several aspects of tropical storm remain speculative. One of the uncertainties, is the distribution of radial motion in the storm inflow layer near the boundary. Aircraft observations of the radial velocity are relatively less accurate because this component has small magnitude. Moreover, the data have been limited to a few flight levels during an individual storm period, which cannot produce an accurate profile of radial winds around a single storm. The vertical variation of radial motion in the inflow layer also cannot be measured. Though the vertical velocity at the top of the boundary layer is very small in comparison with the radial and tangential velocities, it is very significant for the growth and maintenance of a storm.

It is reasonable to suppose that the boundary layer plays an important role in determining the distribution and location of maximum upward motion. Surface friction causes convergence in an area of positive vorticity, and thereby organizes cumulus convection which leads to the development of tropical storm as suggested by Ooyama (1964). In addition, surface friction is important for determining the horizontal scale of the convective area, and in producing the eye and the eyewall as observed in tropical storms.

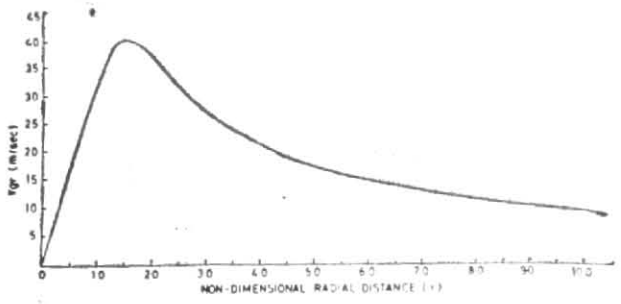

Fig. 1. Tangential velocity profile at the top of the boundary layer

Lency and Rogers (1960) solved the boundary layer equations numerically considering rigid body rotation; but this is not a realistic model for tropical storm winds. Smith (1968) investigated some of the features of tropical storm surface boundary layer by using a momentum integral method. The flow above the friction layer was specified by a suitable pressure profile in gradient balance, and the vertical profiles of tangential and radial velocities were taken as those at geostrophic radius Leslie and Smith (1970) extended the work of Smith (1968) for turbulence represented by different coefficients of eddy viscosity using the same method only in the region outside the maximum tangential velocity. Carrier *et al.* (1971) have pointed out that the momentum integral technique is not accurate enough to predict the vertical velocity at the top of the boundary layer, which is extremely small but a significant quantity.

In our study, the flow above the boundary layer will be represented by a steady inviscid circular vortex with zero radial flow and tangential velocity V_{gr} (R), where, R is the radial distance from the axis of symmetry as shown in Fig. 1. In the absence of horizontal surface boundary, a vortex of this kind can support an arbitrary radial distribution of vertical velocity. But, in the presence of such a boundary, and V_{gr} specified, the upward velocity component (W) is determined uniquely by the boundary layer flow. In this study the dynamics of the boundary layer determined by this external flow are governed by the Navier-Stokes equations of motion. The maximum velocities achieved either in or near the boundary layer are such that the density changes within the boundary layer have negligible effect on the dynamics. At a large distance (about 1000 km or so) from the centre of the storm, the flow can be assumed nearly geostrophic, and at this radius the boundary layer approximates to an Ekman type of layer; but the flow in the core region is nearly like a rigid body rotation. So in this region, boundary layer equations admit separable solution. Keeping in view of these two types of solutions, a method has been developed in this study to find out the boundary layer solutions numerically at different radial distances, starting from the geostrophic radius to the centre of the storm.

There is no unique method to determine the turbulent flow. It is still impossible to analyse different kinds of turbulent flow with the aid of the same hypothesis concerning the turbulent friction. In this study a few expressions for the coefficients of kinematic eddy viscosity based on different hypotheses have been tested and their results discussed.

2. The basic equations

For simplicity, we will assume a steady state. The model is intended to represent a mature and slowly moving storm. We will employ cylinderical co-ordinate R, θ, Z; where, R is the radial distance from the origin, θ is the azimuth and Z is the height above the mean sea level. The model is further simplified by neglecting derivatives with respect to the azimuth distance $\left(\frac{1}{R}\frac{\partial}{\partial\theta}\right)$. This implies an axisymmetric storm. Data indicate that these derivatives are usually small compared to derivatives with respect to the radial distance. In the frame work of boundary layer theory, it is assumed that the same pressure gradient acts in viscous layer near the surface, *i.e.*, the radial pressure gradient is constant with height in the boundary layer. In view of the fact that observations indicate virtually no horizontal gradient of temperature in lower layer of tropical storm (Frank 1977 and others), the assumption regarding constancy of $\frac{1}{\rho}\frac{\partial p}{\partial R}$ with height appears to be fairly realistic for the inflow layer. Under the assumptions, the boundary layer equations for turbulent flow in a rotating frame of reference with a variable eddy coefficients of viscosity are :

$$U\frac{\partial U}{\partial R}+W\frac{\partial U}{\partial Z}-\frac{V^2}{R}-fV+\frac{1}{R}V_{gr}^2+fV_{gr}$$

$$=\frac{\partial}{\partial R}\left\{K_r\left(\frac{\partial U}{\partial R}+\frac{U}{R}\right)\right\}+\frac{\partial}{\partial Z}\left(K_z\frac{\partial U}{\partial Z}\right) \qquad (1)$$

$$U\frac{\partial V}{\partial R}+\frac{UV}{R}+W\frac{\partial V}{\partial Z}+fU$$

$$=\frac{\partial}{\partial R}\left\{K_r\left(\frac{\partial V}{\partial R}+\frac{V}{R}\right)\right\}+\frac{\partial}{\partial Z}\left(K_z\frac{\partial V}{\partial Z}\right) \qquad (2)$$

$$\frac{\partial}{\partial R}(UR)+\frac{\partial}{\partial Z}(WR)=0 \qquad (3)$$

where, U, V and W are the velocity components in the radial, tangential and vertical directions, and 'f' is the Coriolis parameter (5×10^{-5}/sec). According to the assumptions, the pressure gradient term in Eqn. (1) has been replaced by the prescribed tangential velocity field V_{gr} (R) at the top of the friction layer K_r and K_z are eddy coefficients of viscosity in the radial and vertical directions.

2.1. *Boundary conditions*

We will assume a no slip condition at the surface. This implies :

$$U=V=W=0;\quad Z=0 \qquad (4a)$$

and $V=V_{gr}$, $U=0$; $Z=\infty$, *i.e.*, in the free atmosphere where, friction is negligible. (4b)

We assume that the tangential velocity component V has the form : $V = V_{gr} G(r, \eta)$ 5(a)

where, G is a function of non-dimensional radial and vertical distances, r and η.

The radial and vertical velocity components (U and W) may be expressed by a Stoke's stream function Ψ, which is taken as :

$$\Psi = Z_o \, RV_{gr} \, (1+V_{gr}/Rf) \, F(r, \eta) \tag{5b}$$

where, F is a function of r and η; Z_o is a scaling factor for the vertical distance Z, which is being defined shortly.

Using the equation of continuity (3), U and W may be expressed by ;

$$U = V_{gr} (1+V_{gr}/Rf) \frac{\partial F}{\partial \eta} \tag{5c}$$

$$W = -Z_o \left(\frac{dV_{gr}}{dR} + \frac{V_{gr}}{R} + \frac{2V_{gr}}{Rf} \cdot \frac{dV_{gr}}{dR} \right) F - \frac{Z_o}{R} V_{gr} (1+V_{gr}/Rf) \frac{\partial F}{\partial r} \tag{5d}$$

Boundary conditions on G and F, which are consistent with the Eqn. (4) are defined in section 2.2.

The term $(1+V_{gr}/Rf)$ in (5b) is unity plus a local Rossby number. The Stoke's stream function (Ψ) has been assumed in such way that at a large distance from the storm's centre the term V_{gr}/Rf is negligible and the boundary layer equations approximate to an Ekman layer formulation. In the core region, if the super-imposed flow is in rigid body rotation, the boundary layer equations admit separable solutions (Schlichting 1968).

2.2. *Scaling of the variables*

Following scalings are used to make the equations non-dimensional :

$$\begin{aligned} Z_o &= \sqrt{(K_z^*/f)} & K_z &= K_z^* \, k(r, \eta) \\ Z &= Z_o \, \eta & U &= R_o f u \\ R &= R_o \, r & V &= R_o f \, v \\ K_r^* &= R_o^2 f & V_g, &= R_o f v_{gr} \\ K_r &= K_r^* h \, (r, \eta) & W &= Z_o f w \end{aligned} \tag{6}$$

where, $f = (5 \times 10^{-5}/\text{sec})$ is the Coriolis parameter; $R_o = 50$ km (radius of maximum tangential velocity of a typical storm); K_z^* is a characteristic value of vertical eddy coefficient of viscosity, which is taken to be $50 \text{m}^2/\text{sec}$; $K_r^* = (1.25 \times 10^5 \text{m}^2/\text{sec})$ is a characteristic value of radial eddy coefficient of viscosity which has been defined in terms of R_o and f; η and r are non-dimensional vertical and radial distances; u, v, w and v_{gr} are non-dimensional radial, tangential, vertical and super-imposed gradient wind velocity components; $k(r, \eta)$ and $h(r, \eta)$ are non-dimensional vertical and radial components of eddy coefficients of viscosity.

Using (6) and omitting common factors, Eqns. (1) and (2) reduce to the following non-dimensional form with variable coefficients :

$$\begin{aligned} & a_1 \frac{\partial^3 F}{\partial \eta^3} + a_2 \frac{\partial^2 F}{\partial \eta^2} + a_3 \frac{\partial F}{\partial \eta} - a_4 \left(\frac{\partial F}{\partial \eta} \right)^2 \\ & + a_5 F \frac{\partial^2 F}{\partial \eta^2} - a_6 - 1.0 + G + a_8 G^2 + a_7 \frac{\partial^2 F}{\partial \eta \partial r} \\ & + a_8 \left(\frac{\partial F}{\partial r} \frac{\partial^2 F}{\partial \eta^2} - \frac{\partial^2 F}{\partial r \partial \eta} \frac{\partial F}{\partial \eta} \right) = 0 \end{aligned} \tag{7}$$

$$\begin{aligned} & b_1 \frac{\partial^2 G}{\partial \eta^2} + b_2 \frac{\partial G}{\partial \eta} - b_3 \frac{G \partial F}{\partial \eta} + b_4 \frac{F \partial G}{\partial \eta} - b_5 \frac{\partial F}{\partial \eta} + \\ & + b_6 G + b_7 \frac{\partial G}{\partial r} + b_8 \left(\frac{\partial F}{\partial r} \frac{\partial G}{\partial \eta} - \frac{\partial F}{\partial \eta} \frac{\partial G}{\partial r} \right) \\ & + b_9 \frac{\partial^2 G}{\partial r^2} = 0 \end{aligned} \tag{8}$$

where, the coefficients $a_1, \ldots, a_8$ and $b_1, \ldots, b_9$, are functions of one or more of the variables :

$$r, k(r, \eta), h(r, \eta), v_{gr}, \frac{\partial k}{\partial \eta}(r, \eta), \frac{dv_{gr}}{dr} \text{ and } \frac{d^2 v_{gr}}{dr^2}$$

The boundary conditions consistent with those of 4(a) and 4(b) are :

$$\eta = 0 \; : \; G = 0; \quad F = 0 \; ; \; F' = 0 \tag{9a}$$

$$\eta = \infty \; : \; G = 1; \quad F' = 0 \tag{9b}$$

where, prime (′) denotes partial differentiation with respect to η.

3. Numerical procedure

Eqns. (7) and (8) are non-linear. The boundary conditions for F and G, are to be applied at $\eta = 0$, and $\eta = \infty$ (large η). The solutions have natural oscillation making it difficult to obtain an initial guess for the finite difference method. Even for a single differential equation of second order, the two points problem can be troublesome. If the problem is not well behaved, it is usually very difficult or even worthless to apply shooting method (Milne 1970). A finite difference method does have a chance for convergence, as it tends to keep a firm hold

on the entire solutions at once. Considering this, a finite difference method has been used to solve the simultaneous non-linear equations.

We introduce a grid of N intervals of equal step size by choosing N points from $\eta=\triangle\eta$ to $\eta=\triangle\eta N$ in the vertical. The initial conditions at $\eta=0$ and $\eta=\infty$ (Nth point) are introduced directly in the finite difference equations. The non-linear Eqns, (7) and (8) are replaced by linearised finite difference equations for, $i=1,\ldots\ldots\ldots(N-1)$, giving $2N-2$ equations, for $2N-1$ unknowns [since, $G(N)=1.0$]. An extra equation is obtained by taking the derivative of (7) with respect to η, at $\eta=0$, and replaced with finite difference as below :

$$c_1\frac{\partial^4 F(r,0)}{\partial\eta^4}+c_2\frac{\partial^3 F(r,0)}{\partial\eta^3}+c_3\frac{\partial^2 F(r,0)}{\partial\eta^2}+\frac{\partial G(r,0)}{\partial\eta}=0 \qquad (10)$$

where, $c_1=a_1(0)$; $c_2=2a_2(0)$; $c_3=a_2(0)+a_3(0)$

Eqns. (7), (8) and (10) represent a complete set for the solution of the problem, giving $2N-1$ equations for $2N-1$ unknowns.

3.1. *Linearization*

If, F be a dependent variable, and $\bar{F}$ be assumed to be an approximate guess, or a previous step solution, we may set $F=\bar{F}+\epsilon$, where ϵ is the correction required to produce the correct solution F. We need not only ϵ, but also ϵ', ϵ'', ϵ''' and ϵ^{iv}, in order to form the new quantities, $F'=\bar{F}'+\epsilon'$, $F''=\bar{F}''+\epsilon''$ and so on.

The terms like FG', are linearized by putting,

$$FG'=(\bar{F}+\epsilon)(\bar{G}'+\delta')\approx\bar{F}\bar{G}'+\epsilon\bar{G}'+\delta'\bar{F}\ (\text{neglecting}\ \epsilon\delta')$$
$$=F\bar{G}'+\bar{F}G'-\bar{F}\bar{G}' \qquad (11)$$

3.2. *Finite differences*

The differentials, are replaced by following finite, difference scheme :

$$\Phi'_i=(\Phi_{i-2}-8\Phi_{i-1}+8\Phi_{i+1}-\Phi_{i+2})/12s$$
$$\Phi_i''=(-\Phi_{i-2}+16\Phi_{i-1}-30\Phi_i+16\Phi_{i+1}-\Phi_{i+2})/12s^2$$
$$\Phi'''=(-\Phi_{i-2}+2\Phi_{i-1}-2\Phi_{i+1}+\Phi_{i+2})/2s^3$$
$$\Phi_i^{iv}=(\Phi_{i-2}-4\Phi_{i-1}+6\Phi_i-4\Phi_{i+1}+\Phi_{i+2})/s^4 \qquad (12)$$

where, Φ is any variable, 'i' is the grid point and 's' is the grid length.

When the finite difference scheme is applied on the lower boundary, *i.e.*, $\eta=0$, the values of the variables at two grid points below the boundary are required.

Putting the boundary conditions of F and G, at $\eta=0$, first equation of motion (7) reduces to :

$$k(r,0)F'''(r,0)+\frac{\partial k}{\partial\eta}(r,0)F''(r,0)-1=0 \qquad (13)$$

Expanding F in the neighbourhood of $\eta=0$ (at $\eta=\pm\triangle\eta$ and $\pm2\triangle\eta$) by a Taylor series and putting the boundary condition of F, the values of $F''(r,0)$ and $F'''(r,0)$ can be obtained in terms of F_1, F_2, F_{-1}, F_{-2}, and $\triangle\eta$. Replacing the differentials in (13) with these finite differences, we get :

$$F_{-1}=ca\,F_1-cca$$
$$F_{-2}=cb\,F_2-ccb \qquad (14)$$

where, ca, cca, cb, ccb are functions of $k(r,0)$, $\frac{\partial k}{\partial\eta}(r,0)$ and $s\ (=\triangle\eta)$.

Putting the boundary conditions of F and G, at $\eta=0$ in second equation of motion (8), we get :

$$G''(r,0)+pG'(r,0)=0$$

where, $p=\frac{\partial k}{\partial\eta}(r,0)/k(r,0)$

In the neighbourhood of $\eta=0$, G has a solution of the form :

$$G=1.0-e^{-p\eta}$$

Expanding the exponent at $\eta=\pm\triangle\eta\ (=\pm s)$; and $\eta=\pm2\triangle\eta\ (=\pm2s)$; and since $|ps|\gg1.0$; after, simplification, we get :

$$G_{-1}=-G_1+p^2s^2+p^4s^4/12+\ldots\ldots \qquad (15a)$$
$$G_{-2}=G_2+4p^2s^2+4p^4s^4/3+\ldots\ldots \qquad (15b)$$

Beyond the upper boundary ($i=N$), the values of F and G are also required at the point $i=N+1$. Using boundary conditions, these can be taken as :

$$F_{N+1}=-10F_N/3+6F_{N-1}-2F_{N-2}+F_{N-3}/3$$
$$G_{N+1}=1.0 \qquad (16)$$

Finally, applying linearization method (11), finite difference scheme (12) and relations, (14), (15) and (16); Eqns. (7) and (8) can be expressed by the following difference form at the grid point 'i' :

$$\theta_iF_{i-2}+\alpha_iF_{i-1}+\beta_iF_i+\gamma_iF_{i+1}+\delta_iF_{i+2}+\xi_iG_i=\lambda_i \qquad (17)$$

$$e_iF_{i-2}+g_iF_{i-1}+l_iF_i+c_iF_{i+1}+d_iF_{i+2}+m_iG_{i-2}+p_iG_{i-1}+q_iG_i+r_iG_{i+1}+\eta_iG_{i+2}=t_i \qquad (18)$$

for, $i=1, 2, 3 \ldots\ldots\ldots N-1$. Similarly, Eqn. (10) reduces to :

$$cb_1F_1 + cb_2F_2 + cb_3G_1 + cb_4G_2 = cb_5 \qquad (19)$$

where the coefficients $\theta_i, \alpha_i, \beta_i, \gamma_i, \delta_i, \xi_i, e_i, g_i, l_i, c_i, d_i, m_i, p_i, q_i, r_i, \eta_i, (i=1, N-1)$; cb_1, cb_2, cb_3, cb_4; and right hand side $\lambda_i, t_i\,(i=1, N-1)$ and cb_5 are functions of one or more of the following variables:

$$r,\ v_{gr},\ k(r, \eta),\ h(r, \eta),\ \bar{F}(r, \eta) \text{ and } \bar{G}(r, \eta)$$

Eqns. (17), (18) and (19) have $2N$-1 equations for $2N-1$ unknowns ($F_1, F_2, F_3 \ldots\ldots\ldots F_N$; $G_1, G_2, G_3 \ldots\ldots G_{N-1}$); which are solved at each step by a direct method using double precision arithmetic. In our numerical calculations, $N=40$; so, 79 equations are solved at a time.

At geostrophic radius (large r), first step initial values of F and G are taken from the known Ekman layer solutions, *i.e.*,

$$F = [e^{-\eta/\sqrt{2}}\,(\cos \eta/\sqrt{2} + \sin \eta/\sqrt{2}) - 1]/\sqrt{2},$$

and $G = 1 - e^{-\eta/\sqrt{2}}\,(\cos \eta/\sqrt{2})$

At successive steps (at same r), F and G are taken from previous step solutions. The process is repeated until the variations of F and G at consecutive steps at each point of η become negligible. At the next smaller value of r, the initial guesses for F and G are taken from the previous step solutions and the same process is repeated until the solutions converge. Repeating the process, solutions up to the nearest point of storm's centre are obtained.

4. Numerical experiment

We feel that a more quantitative description of the structure of turbulence is needed for a satisfactory formulation of the inflow layer. This could be achieved after more observations become available, but in absence of sufficient data, it is better to test different semi-empirical hypothesis and compare with available informations.

One of the objectives of this study is to investigate how the turbulent structure could be represented in the boundary layer. The following different formulations of the eddy coefficient of viscosity for turbulent flow are tested and compared with available informations.

4.1.1. *Constant K_z (Case A)*

The simplest way to study the turbulent flow is to represent it by a constant kinematic eddy coefficient of viscosity K_z, as in laminar flow. In this case, it is difficult to estimate what should be the proper value of K_z. A value of the order of 50m²/sec was suggested by budget studies of hurricanes by Kasahara (1961) and Syono (1951), Rosenthal (1962), Smith (1968) and Haurwitz (1936) used the same value. But, some assume a value as low as 10m²/sec, while other consider a value in the range of 100-150m²/sec. Here, we put $K_z=50$ m²/sec, with no variation in the radial or vertical direction.

4.1.2. *Variable K_z (Case B)*

Since eddy viscosity is not a property of fluid like viscosity of Stoke's law in laminar flow; but depends upon itself on the mean flow. It was unlikely that K_z could be regarded as a constant over the whole extent of the storm. Prandtl hypotheses that lumps of fluid on the whole preserve their velocity in turbulent motion, and hence their momentum in the principal flow direction. According to his hypothesis the coefficient of kinematic eddy viscosity $K_z = l^2(\partial V/\partial Z)$, where V is the velocity of mean motion and 'l' is mixing length, which is unknown. It is known from experimental evidence that turbulent drag is roughly proportional to the square of velocity and the same result is obtained from Prandtl's hypothesis, if mixing length is assumed to be independent of magnitude of the velocity. This consideration leads us to take K_z proportional to V_{gr}. So we put $K_z=1.25$m. V_{gr} with no vertical variation. The choice of constant (1.25m) is to make the maximum value of $K_z=50$m²/sec, where V_{gr} becomes 40m/sec.

4.1.3. *Exponential vertical variation of K_z (Case C)*

Under neutral stability and for moderate wind speed (less than about 15m/sec), it is well established observationally that $K_z=kv^*z$ in the sub-layer, where shearing stress remains constant. The height of this layer ranges from 50-200 m. In this formula k is Vonkarman's constant which is approximately 0.4 and v^* is friction velocity defined in terms of the surface stress τ_o by $v^* = |\tau_o/\rho|$. At a larger height, the variation of K_z with z is an open question, but one can say that the variation is much slower than in the sub-layer. Moreover, K_z cannot increase indefinitely. Consequently, we put $K_z = K_z^*[1\text{-}\exp(-kv^*z/K_z^*)]$, where $k=0.4$ and $v^*=.5$m/sec. With this representation, K_z varies nearly linearly with height near the surface, and less rapidly with increasing height. At large height, it will approach to 50m²/sec. In this case, there is no radial variation of K_z.

4.1.4. *Radial and vertical variation of K_z (Case D)*

Here, K_z is considered from Prandtl's mixing length hypothesis as discussed in Sec. 4.1.2, with a constant mixing length and variation of $\partial V/\partial Z$ in the boundary layer. In addition, a constant value is added to it, so that at the top of the boundary layer, K_z does not become very insignificant, where $\partial V/\partial Z$ is very small. Thus, we put $K_z=25\text{m}^2/\text{sec}+10^3\text{m}^2\,\partial V/\partial Z$. Anthes (1977) in his numerical model for hurricane, used such an expression for K_z from empirical consideration. Here, K_z, will vary both radially and vertically.

4.2. *External flow above the boundary layer*

The external flow above the boundary layer is assumed to be axisymmetric and in gradient balance without any radial flow. In a tropical storm, one does not know the exact swirl distribution and it need not be the same for all storms. However, it is sufficient to take a profile

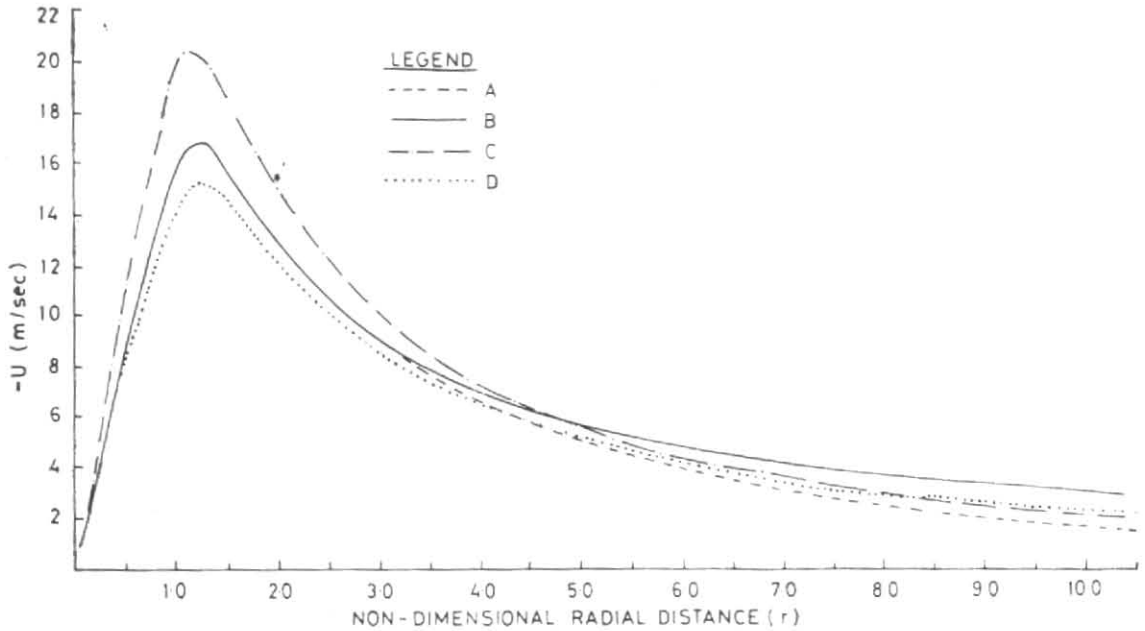

Fig. 2. Radial profiles of maximum inflow velocity U

which has the general form of those observed in a typical tropical storm. Rosenthal (1962) and Smith (1968) derived the velocity profile of the external flow by assuming a suitable pressure profile in gradient balance. In this problem the profile has been taken from Mandal's (1988) model of a tropical storm from temperature anomaly field. Fig. 1 shows its variation with radial distance, r. It increases rapidly from zero at the centre to the maximum value of 40.5m/sec at $r=1.4$ ($R=70$km), and then decreases gradually with increasing r to about 5m/sec at $r=16.0$ ($R=800$ km). In the core region, the profile has slightly been modified to represent exact rigid body rotation up to $r=0.9$. This enables us to to compare the behaviour of our solutions with those of rigid body rotation. In this profile, the relative vorticity remains constant (136×10^{-5}/sec) up to $r=0.9$, then decreases slowly and becomes very small beyond $r=3.0$.

4.3. *Grids and numerical computations*

From the Thermodynamic consideration, Palmen and Riehl (1957) concluded that the inflow must be restricted to the lower 3 km of the storm. This conclusion is consistent with the mean hurricane composite obtained from a standard data network by Jordan (1952) and Miller (1958). Anthes (1982) pointed out that the strongest inflow occurs within an elevation of about 500m; although weak inflow often occurs at an elevation of about 3 km or more. The radial wind component is a significant component of flow below 1.0 km. Carrier *et al.* (1971) with their work beyond the core region of storm, have shown that thickness of inflow layer is of the order of 1.6 km with an outflow layer of very weak radial velocity above it. Frank (1977) in his composite studies of hurricanes mentioned that there is a cyclonic maximum between 900 and 800 mb (hPa), at the effective top of the friction boundary layer. It is possible that mid-level inflow results from an upward extension of frictional convergence by cloud momentum fluxes or from net entrainment into deep clouds.

In our numerical calculations, we have fixed the upper boundary of integration at a height of 1.6 km ($\eta=1.6$) with equal grid spacing of 40 grid points, which reduces the grid length $\triangle\eta$ to 0.04. In radial direction the grid length is variable. From outer region, it is decreased step by step to the centre of the storm.

In tropical storm the ratio of its vertical scale to horizontal scale is very small; in consequence of it, the horizontal gradients of the stress terms are much smaller than the vertical gradients. So, in the present study the radial coefficient of eddy viscosity will not be considered for numerical calculation. It will be considered in the next study.

5. Results and discussion

Fig. 2 shows the radial variations of maximum (at a particular, r) inflow velocity for four cases. These occur at different heights at different radial distances. In all cases, the radial velocity increases with decreasing radius, slowly at first and then more rapidly as the region of maximum tangential velocity is approached; thereafter, it decreases sharply to zero at the centre. These are characteristic profiles of inflow winds associated with a moderate storm. Its highest value shifts slightly to the centre from the maximum superimposed velocity. This shifting may be the result of an inward turbulent transfer of angular momentum from higher wind region. In A and B, it has same value of 16.8m/sec; while it is smallest (15.3m/sec) in D and largest (20.5m/sec.) in C. Far away from the centre, A has lesser value than B; C and D are in between them. In B, it is nearly one third of the superimposed velocity V_{gr}.

The variation of maximum radial velocity with the same external flow can probably be explained by comparing it with experimental results of laminar flow. In laminar flow, the boundary layer thickness of rotating fluid on solid surface is proportional to $\sqrt{(K_z/\Omega)}$,

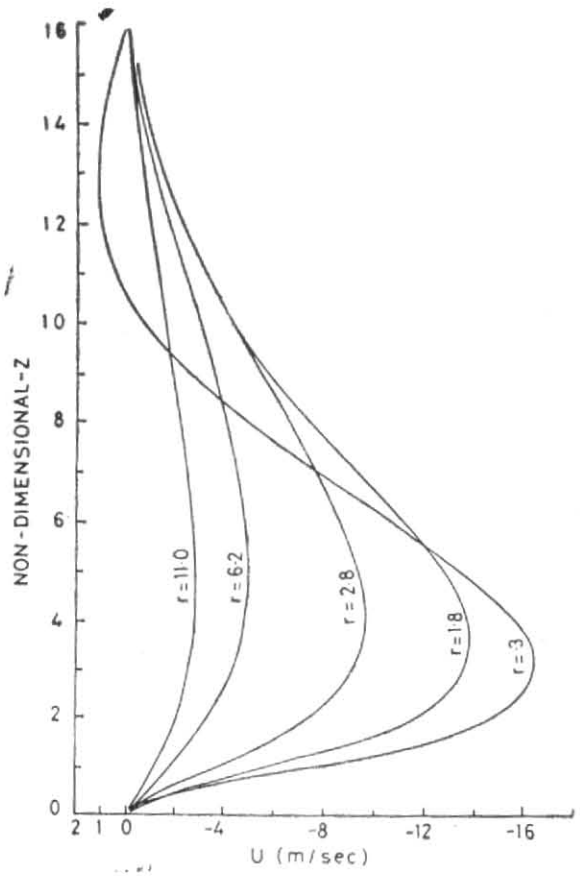

Fig. 3. Vertical profiles of U at different radial distances, case B

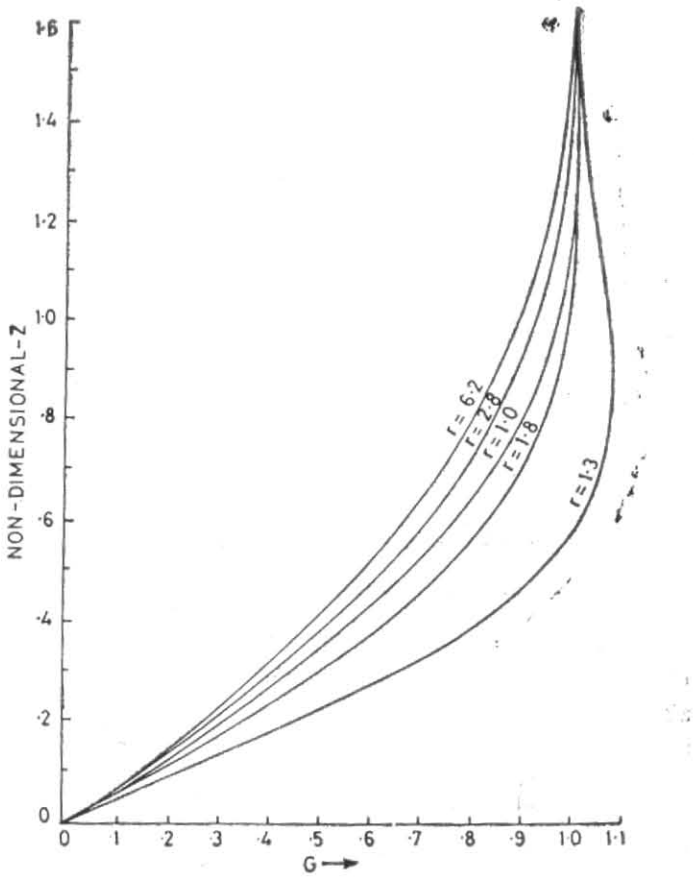

Fig. 4. Vertical profiles of G, case B

where Ω is the angular velocity of external flow (Schlichting 1968). With same Ω, if the value of K_z is smaller, the change of V from zero at the surface, asymtotically to V_{gr} at higher level, takes place through smaller depth than with larger K_z. But, as in case C, if K_z increases with height, the value of V will remain appreciably lower than V_{gr} through greater depth than with constant K_z. Thus the radial inflow which is caused by the deficit of centrifugal force in the rotational component of velocity, will continue to maintain its increasing tendency to higher level causing higher value. Higher maximum value of U in C than in A, may probably be due to this reason. Lower value in D, can be argued in a similar way.

The maximum values of U obtained in cases A, B and D appear to be consistent with those found in other models and real storm. In Smith's (1968) model with maximum superimposed velocity of 40m/sec, same surface boundary conditions and with constant K_z as in A, maximum inflow velocity was 15.25 m/sec; while in Rosenthal's (1962) model with maximum superimposed velocity of 46m/sec and different surface boundary condition, but with same value of K_z, maximum inflow velocity was slightly more than 14m/sec. Anthes (1982) has pointed out that for a wind speed of 50m/sec and typical cross isobaric flow angle of 25 degree, the radial component would be 21m/sec.

The radial velocity varies with height and radial distance. Fig. 3 shows the variation of U with height at different radial distances in B. The profiles away from the centre are more flat and gradually become steeper as the radial distance decreases. The variation is steeper near the surface boundary as would be expected. At higher levels, it slowly decays to a vanishing value. The height of maximum value also decreases with decreasing radial distance. In the core region, there is a weak outflow above the inflow region ($r=1.3$). Composite studies by Shea and Gray (1973) support this. Extremely low sea level pressure in the centre of a fully developed storm far exceeds the value that could be caused by the hydrostatic effect of the temperature rise in the wall cloud by the release of latent heat of condensation. The development of the central eye with its considerably higher temperature is, therefore, due to other effects. This could be due to the subsidence caused by the radial outflow of air in the lower level during deepening process. Gray and Shea (1973) mentioned that very strong horizontal wind shear at the boundary of the eye and eye wall region induces a high degree of turbulent mixing and horizontal momentum transfer into the eye where pressure gradient is small. The winds on the inner edge of the eye, thus must become supergradient and be accelerated outward into the wall clouds, inducing sinking of air from higher levels and warming in the eye.

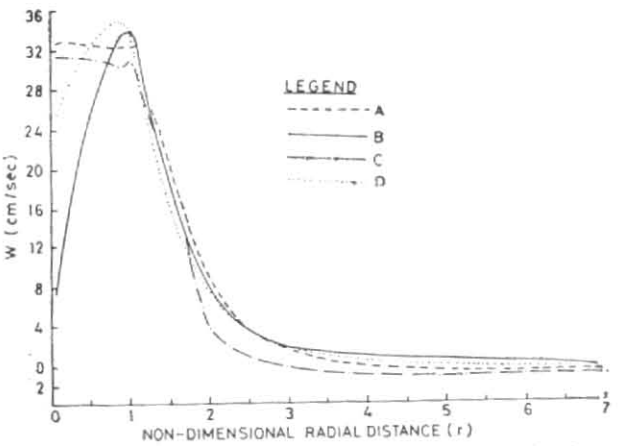

Fig. 5. Vertical motion at the top of the inflow layer

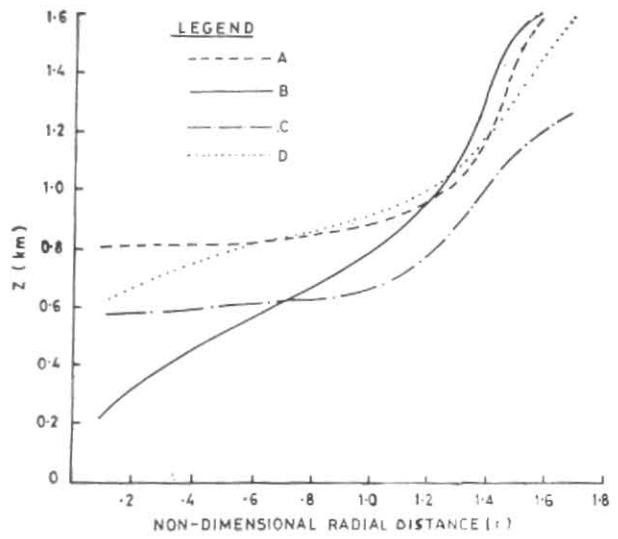

Fig. 6. Depth of inflow layer near the core

The vertical variation of G, and hence that of V at different radial distances are shown in Fig. 4. Here also, the variation is steeper near the surface and tends asymptotically to unity at higher level. In the upper part of the core region, the value of G exceeds unity. As discussed in previous paragraph, this may be due to horizontal momentum transfer into the eye.

The profiles of vertical velocity W, at the top of the inflow layer for the four cases A, B, C and D are shown in Fig. 5. The circumferential velocity distribution in the boundary layer must transport fluid radially inwards and the fluid must be supplied by a very slow downward motion in the exterior region. In all cases, there is a large region of slowly varying weak downdraft surrounding a small region of updraft around the centre. The updrafts are strongest close to and slightly inside of maximum tangential velocity. The downdraft extends from the edge of the storm, gradually increases with decreasing radius, then again decreases and becomes an updraft. Up to 125km the updraft is very small; but inward of this position, it increases very sharply. The maximum value of downdrafts in cases A, B, C and D are —0.65, —0.25, —0.52 and —0.25 cm/sec respectively. In Carrier *et al.* (1971) work for exterior region (K_z = 10m²/sec) it was —0.26 cm/sec; while in Smith's (1968) model (Kz=50m²/sec), it was —0.50 cm/sec. In A and C, the maximum upward velocity in the core region remains nearly constant with decreasing r; while in B and D, after attaining highest value it decreases towards the centre, more sharply in B than in D. The depth of the inflow layers in the core region are shown in Fig. 6. In A, the maximum value of W is 32.5 cm/sec with nearly constant thickness of the inflow layer in the core; the case C is nearly of the same type, but with lesser values. In B, the maximum value of W is 34.5 cm/sec. Both W and thickness of the inflow layer gradually decreased towards the centre. In D, the maximum value of W is 35.2 cm/sec, which is the highest of all cases. The inflow layer also decreases towards the centre but less rapidly than B. The variation of W and the thickness of the inflow layer in the core region in all cases seem to be consistent with the variation of the coefficients of eddy viscosity.

The motion near a stationary wall, when the fluid at a large distance above it rotates with constant angular velocity and constant viscosity are discussed in Schlichting (1968). It is found that the vertical velocity component, W does not depend upon the radial distance r, and at all points it is upward. In this study the angular velocity of the superimposed flow is nearly constant in the core region, and in A we have got same type of results as above. In Rosenthal's (1962) model, with same K_z and boundary condition as in A, and maximum absolute vorticity $\zeta = 650 \times 10^{-5}$/sec, the maximum upward velocity was 22 cm/sec near the maximum superimposed velocity, V_{max} (46m/sec). In Smith's (1968) model, it was more than 100cm/sec at a distance of 13km from the centre with $\xi = 205 \times 10^{-5}$/sec and V_{max}=40m/sec at 40 km from centre. In Leslie and Smith's (1970) model, with K_z=7.8m²/sec, and same V_{gr} profile as in Smith's, maximum W was 37 cm/sec, far inside the core from V_{max}.

It has already been mentioned that Smith (1968) and Leslie and Smith (1970) used a momentum integral method. Frank (1977) in composite studies of hurricane pointed out that the vertical velocity at a radius of 1-degree from the centre and at a height of 950 mb was about 400 mb/day (≈ 4.5 cm/sec). Gray and Shea (1973) computed the vertical motion kinematically utilising divergence from composite studies above 900 mb. The largest ascending vertical motion was of the order of 80 cm/sec above 650 mb. It was concentrated in a narrow zone around the radius of maximum wind. Just above 900 mb, it was of the order of a few cm/sec. This pattern supports the view, first mentioned by Wexler (1947) and later emphasised by Hughes (1952), Simpson (1952) and others, that a large fraction of ascending motion often occurs through a relatively narrow ring near the storm's centre. A study by Riehl and Malkus (1961) indicates that the hurricanes does not have a uniform vertical motion pattern; only a small portion of the inner core is covered by a strong updraft. From the results of Malkus *et al.* (1961), it was estimated that only 4% of the inner rain band area between 10 & 100 km radii had hot towers with 10m/sec updraft near the tower top. Anthes (1982) pointed out that the vertical velocity at the cloud base is considerably larger than the mean vertical velocity. If updraft of a cloud base covers 5% of the area and there is no subsidence between the clouds, then the cloud base vertical velocity for a mean value W of 2.7 cm/sec would be 54 cm/sec. In reality, air is subsiding between clouds, so that cloud base vertical velocity would be greater.

The inflow angles at the surface for four cases are shown in Fig. 7. In all cases, the inflow angle is small at large radii; it gradually increases with decreasing radius and becomes maximum outside the region of maximum velocity, then it decreases rapidly at different rates. In the central core, it decreases slowly or remains nearly constant. In case C, it is too large throughout the entire storm area. In the outer region, the variation is more in A than in B or D. In the core region, the rate of decrease with radius is more in B than in A; while in D, it is nearly constant. The maximum inflow angle in A and B is 34-degree; but in D it is 31 degree. The variation in different cases may be attributed to the variation of the eddy coefficient of viscosity near the surface. The maximum inflow angle in Rosenthal's (1962) model was about 33-degree. Frictional convergence enhances the convective heating and this increases the convergence through modification of the pressure field. Consequently, one might expect that frictional

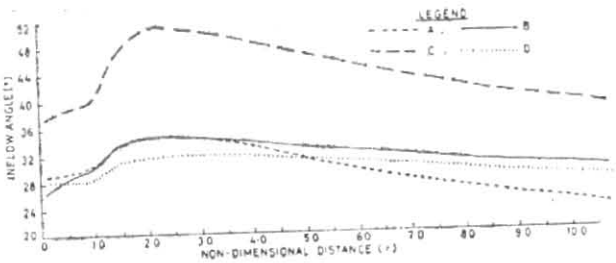

Fig. 7. Surface inflow angle as a function of radius

convergence is relatively large in the inner part of the convective area, except near the storm centre. Inflow angle in B, appears to be consistent with reality.

6. Conclusions

It is evident from our results that the magnitude and distribution of induced meridional circulation depends upon the structure of turbulence. In the core region, if K_z is constant both radially and axially, the upward velocity W does not decrease from its maximum value towards the centre. This is not consistent with the existence and favourable for creation of an eye of a tropical storm. If K_z increases from surface with height, but does not vary with radius, both the radial velocity and inflow angle become too high and in the core region W does not decrease to the centre. On the other hand, if the eddy coefficient of viscosity is assumed to vary with the superimposed flow above the boundary layer, the solutions compare favourably well with observations including inflow angle and boundary layer thickness. One of the important results of this study is that it can simulate the outflow in the core region of boundary layer which is essential for creation of an eye. Though the vertical velocity is a very small quantity in comparison with other components, its magnitude and distribution is very significant for the growth and maintenance of tropical storms. It seems that this model can simulate it well. This model can be used to study the boundary layer of a tropical storm from outer region to the centre of the storm without neglecting non-linear terms in equations of motion. Moreover, there is no necessity of assuming any velocity profile, as required in momentum integral method. Representation of different kinds of boundary layer flow in the interior and exterior regions of a storm by a single Stoke's stream function as developed in this study seems to be consistent with the physical process of real storm. Finally, the finite difference method applied here, can be used to solve other non-linear simultaneous differential equations.

On the sea surface, only the no-slip boundary conditions of the variables have been tested. Further studies are to be made incorporating suitable surface stress terms.

Acknowledgements

The author wishes to express his gratitude to Dr. Ambarish Ghosh, Professor, Indian Statistical Institute, Calcutta for his encouragement and guidance throughout the study. He also expresses his sincere thanks to Director General of Meteorology, India Meteorological Department, New Delhi for providing computer facilities.

References

Anthes, R.A., 1977, "Hurricane model experiments with a new cumulus parameterization scheme", *Mon. Weath. Rev.*, **105**, pp. 287-300.

Anthes, R.A., 1982, "*Meteorological Monographs*", Tropical cyclones, their evaluation, structure and effects, **19**, No. 4.

Carrier, G.F., Hammond, A.L. and George, O.D., 1971, "A model of the mature hurricane", *J.F. Mech.*, **47**, pp. 145–170.

Frank, W.M., 1977, "The structure and energetics of tropical cyclone I—Storm structure", *Mon. Wealth. Rev.*, **105**, pp. 1119–1135.

Gray, W.M. and Shea, D.J., 1973, "The hurricane inner core region–II. Dynamic and thermodynamic characteristics", *J. Atmos. Sci.*, **30**, pp. 1565–1576.

Haurwitz, B., 1936, "On the vertical wind distribution in anticyclones, extra tropical and tropical cyclones under influence of eddy viscosity", *Beitrage zur Geophys.* **47**, pp. 206–214.

Hughes, L.A., 1952, "On the low level wind structure of tropical cyclones", *J. Met.*, **9**, pp. 442–448.

Jordon, E.S., 1952, "An observational study of the upper wind circulation around tropical storms", *J. Met.*, **9**, pp. 340–346.

Kasahara, A., 1961, "A numerical experiment on the development of tropical cyclones", *J. Met.*, **18**, pp. 259–282.

Lancy, G.N. and Rogers, M.H., 1960, "The rotating symmetric flow of a viscous fluid in presence of an infinite rotating disc", *J.F. Mech.*, **7**, pp. 617–631.

Leslie, L.M. and Smith, R.K., 1970, "The surface boundary layer of a hurricane", *Tellus*, **22**, pp. 288–296.

Malkus, J. Ronne, C. and Chafee, M., 1961, "Cloud patterns in hurricane (*Daisy* 1958)", *Tellus*, **13**, pp. 8–30.

Mandal, J.C., 1988, "A model of tropical storm from temperature anomaly distributions", *Mausam*, **39**, pp. 367–374.

Miller, B.I., 1958, "The three-dimensional wind distribution around a tropical cyclone", *Nat. Hurr. Res. Proj. Rep.* No. 15, p. 41.

Milne, W.E., 1970, "*Numerical solution of differential equations*, Dover Publications, Inc., New York. p. 102.

Ooyama, K., 1964, "A dynamical model for the study of tropical cyclone development", *Geofisica International* (Mexico), **4**, pp. 187–198.

Palmen, E., and Riehl, H., 1957, "Budget of angular momentum and energy in tropical cyclones", *J. Met.*, **14**, pp. 150–159.

Riehl, H. and Malkus, J.S., 1961, "Some aspects of hurricane *Daisy* (1958)", *Tellus*, **13**, pp. 181–213.

Rosenthal, S.L., 1962, "A theoretical analysis of the field of motion in the hurricane boundary layer", NHRP Report No. 56.

Schlichting, H., 1968, "*Boundary Layer Theory*", p. 213.

Shea, D.J. and Gray, W.M., 1973, The hurricane's inner core region. I-Symmetric and asymmetric structure. *J. Atoms. Sci.*, **30**, pp. 1544–1564.

Simpson, R.H., 1952, "Exploring the eye of typhoon *Marge*, 1951", *Bull. Amer. met. Soc.*, **33**, pp 286–298.

Smith, R.K., 1968, "The surface boundary layer of a hurricane", *Tellus*, **20**, pp. 473–484.

Syono, S., 1951, "On the structure of atmospheric vortices", *J. Met.*, **8**, pp. 103–110.

Wexler, H., 1947, "Structure of hurricane as determined by radar", *Ann. N.Y. Acad. Sci.*, **48**, pp. 821–844.